Selected papers presented at the 14th Symposium of Magnetic Measurements and Modelling SMMM'2023

Structure and Magnetic Properties of the Magnetocaloric MnCoGe Modified by W

K. Kutynia, A. Przybył and P. Gębara*

Department of Physics, Częstochowa University of Technology, Armii Krajowej 19, 42-200 Częstochowa, Poland

Doi: 10.12693/APhysPolA.146.70 *e-mail: piotr.gebara@pcz.pl

The investigation of the nonmagnetic W-substitution effect on the structure and magnetocaloric properties of the MnCoGe alloy was conducted. The analysis of phase composition revealed the coexistence of a hexagonal Ni_2In-type phase and an orthorhombic TiNiSi-type phase. A detailed analysis of XRD patterns supported by Rietveld analysis showed changes in the lattice constants and the content of recognized phases, which depended on the W content in the alloy. A monotonic decrease in the Curie temperature with an increase in W content in the alloy composition was noticed. The values of ΔS_M measured for the variation of the external magnetic field ~ 5 T were equal to 5.30, 4.16, 2.32, and 3.01 for $Mn_{0.97}W_{0.03}CoGe$, $Mn_{0.95}W_{0.05}CoGe$, $Mn_{0.93}W_{0.07}CoGe$, and $Mn_{0.9}W_{0.1}CoGe$ alloy, respectively. The analysis of n vs T curves recovered for the tested alloys was characteristic of second-order phase transition.

topics: magnetocaloric effect, MM'X alloys, X-ray diffraction (XRD)

1. Introduction

Magnetic cooling is a phenomenon based on the magnetocaloric effect (MCE) and is a more environmentally friendly method of lowering temperature than conventional cooling techniques. This phenomenon has been known to mankind for over a hundred years, but we are still looking for ideal magnetocaloric materials that can be used commercially. The magnetocaloric effect is described as an adiabatic temperature change (ΔT_{ad}) or an isothermal change in magnetic entropy (ΔS_M). This phenomenon was discovered in 1881 by Warburg [1] and described in more detail independently by Debye in 1926 [2] and Giaugue in 1927 [3], but only thanks to research conducted by Pecharsky and Gschneidner Jr. in 1997 [4], the number of publications related to the topic of magnetocaloric materials increased exponentially. Currently, alloys are sought that are relatively cheap but also have the desired properties (large change in magnetic entropy ΔS_M and appropriate Curie temperature T_C).

At present, many scientists are focusing on MnCoGe alloys belonging to the group of MM'X alloys (where M or M' is a transition metal and X — a metalloid), which are characterized by excellent magnetocaloric properties. MM'X alloys crystallize in two phases: a high-temperature hexagonal phase of the Ni_2In-type (space group $P6_3/mmc$) and a low-temperature orthorhombic phase of the TiNiSi-type (P_{nma}) [5]. The magnetic moments of MM'X alloys are strongly related to the crystal structure because they cause magnetic transitions to be associated with discontinuous changes in the crystal symmetry as well as lattice parameters. Thanks to this feature, these alloys can exhibit gigantic MCE around the occurring first-order magnetostructural phase transitions [6].

Our previous articles based on MnCoGe alloys were based on partial substitution of Zr [7] and Pd [8] dopants. These changes improved the value of the magnetic entropy change and also increased the Curie temperature. Taking into account the research results described in [9], we decided to investigate the influence of the W dopant on the structure and magnetocaloric properties of $Mn_{1-x}W_xCoGe$ (where $x = 0.03$, 0.05, 0.07, and 0.1).

2. Sample preparation and experimental details

The ingot samples were prepared by arc-melting of high-purity constituent elements under low pressure of Ar. Compositions were established as follows: $Mn_{0.97}W_{0.03}CoGe$, $Mn_{0.95}W_{0.05}CoGe$, $Mn_{0.93}W_{0.07}CoGe$, and $Mn_{0.9}W_{0.1}CoGe$. Samples were remelted ten times in order to ensure their homogeneity. The structural study was based on X-ray diffraction and was carried out using a Bruker D8 ADVANCE diffractometer with Cu K_α radiation. Qualitative and quantity analysis was supported by

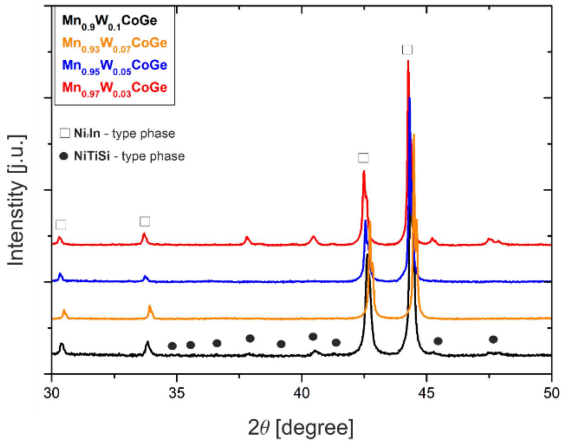

Fig. 1. The X-ray diffraction patterns collected at room temperature for samples of produced alloys.

Bruker EVA 4.0 software and PowderCell 2.4 package for the Rietveld refinement [10]. The magnetic properties (i.e., the Curie temperature and magnetic isotherms) were investigated using the Quantum Design Physical Properties Measuring System (PPMS) Model 6000, working over a wide range of magnetic fields and temperatures. In order to check structural transformation, the differential scanning calorimetry (DSC) curves were collected using a differential scanning calorimeter NETZSCH 214 Polyma (Selb, Germany) with a heating and cooling rate of 10 K/min. The microstructural observations were registered using scanning electron microscopy (SEM) JEOL 6610LV equipped with energy dispersive X-ray spectrometer (EDS).

3. Results and discussion

Figure 1 shows the XRD patterns of all tested $Mn_{1-x}W_xCoGe$ samples (where $x = 0.03$, 0.05, 0.07, and 0.1). The analysis revealed two different phases in the studied series of samples: dominant hexagonal Ni_2In phase and minor orthorhombic NiTiSi phase. During the analysis, reflexes corresponding to the orthorhombic NiTiSi-type phase were clearly visible for samples with $x = 0.03$ and 0.1. In the case of samples with $x = 0.05$ and 0.07, traces of this phase were detected. Moreover, the highest content of volume fraction of the NiTiSi-type phase with a minor Ni_2In-type phase for the $Mn_{0.9}W_{0.1}CoGe$ alloy was detected.

The calculations of the lattice constant for the recognized phases showed its monotonic rise with an increase in W in each sample. Such an effect is related to the different ionic radius of W ($r_W = 1.41$ Å) compared to a much lower Mn radius ($r_{Mn} = 1.18$ Å). In the work of Bażela et al. [11], the orthorhombic cell was treated as a distorted hexagonal cell, therefore in the case of the W atom, it affects the distortion of the cell and also favors the crystallization of the hexagonal Ni_2In-type phase, which is not desirable, taking into account magnetocaloric properties. A detailed examination of X-ray diffractograms excluded contamination with additional phases. The conclusions from the quantitative and qualitative analysis were supported by the Rietveld improvements, and the results are presented in Table I.

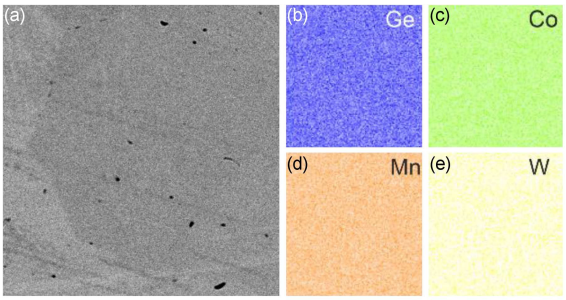

Fig. 2. The SEM micrograph (a) and corresponding EDS maps of the $Mn_{0.95}W_{0.05}CoGe$ alloy sample (b–e).

TABLE I

Data delivered by the Rietveld analysis for the investigated $Mn_{1-x}W_xCoGe$ alloy samples.

Alloy	Recognized phases	Lattice constant [Å] ±0.001	Volume fraction [%]
$Mn_{0.97}W_{0.03}CoGe$	hex Ni_2In-type	$a = 4.071$ $c = 5.284$	83
	ort NiTiSi-type	$a = 5.933$ $b = 3.819$ $c = 7.049$	17
$Mn_{0.95}W_{0.05}CoGe$	hex Ni_2In-type	$a = 4.073$ $c = 5.287$	93
	ort NiTiSi-type	$a = 5.937$ $b = 3.821$ $c = 7.051$	7
$Mn_{0.93}W_{0.07}CoGe$	hex Ni_2In-type	$a = 4.075$ $c = 5.286$	94
	ort NiTiSi-type	$a = 5.939$ $b = 3.824$ $c = 7.053$	6
$Mn_{0.9}W_{0.1}CoGe$	hex Ni_2In-type	$a = 4.079$ $c = 5.292$	92
	ort NiTiSi-type	$a = 5.943$ $b = 3.828$ $c = 7.061$	8

The microstructure of the samples was observed using the SEM technique. Fragment of the microstructure of the $Mn_{0.95}W_{0.05}CoGe$ sample is shown in Fig. 2a. The EDS maps collected for the tested sample microstructure show a uniform distribution of the components (Fig. 2b –e), which was expected based on previous studies presented in [8]. The concentration of nominal composition, i.e.,

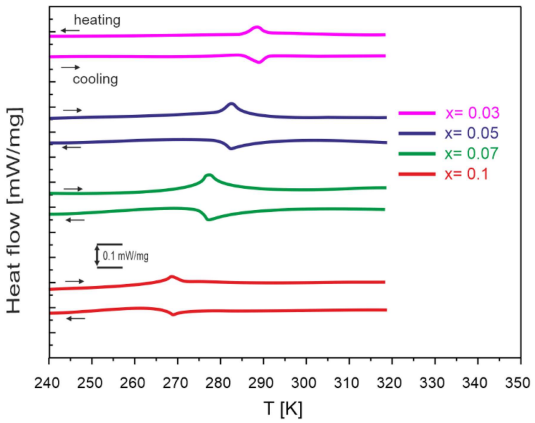

Fig. 3. The DSC curves and temperature dependences of magnetization (field cooling regime at $\Delta(\mu_0 H) = 0.1$ T).

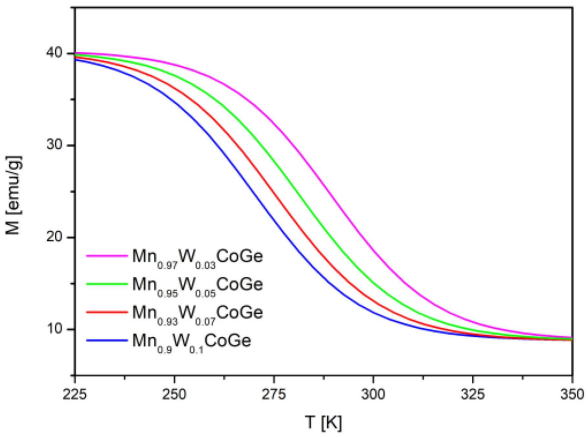

Fig. 4. The temperature dependences of magnetization collected under the external magnetic field of 0.1 T for all studied samples.

Mn — 31.67 at.%, W — 0.02 at.%, Co — 33.33 at.%, and Ge — 33.33 at.%, corresponds well with the values obtained by EDS measurement, i.e., Mn — 31.52 ± 0.22 at.%, W — 0.95 ± 0.18 at.%, Co — 33.2 ± 0.25 at.%, and Ge — 34.33 ± 0.36 at.%, respectively.

The DSC measurements performed for W-doped MnCoGe alloys are summarized in Fig. 3. DSC tests were performed to confirm the results of XRD analysis and to determine the temperatures of structural and magnetic transitions. Endothermic and exothermic peaks are present in all tested samples. The lambda-type peaks were detected for all studied samples in the vicinity of 282 K and 277 K for $Mn_{0.95}W_{0.05}CoGe$ and $Mn_{0.93}W_{0.07}CoGe$ alloy, respectively. The presence of lambda peaks in DSC curves suggests an occurrence of second-order phase transition in investigated specimens.

In order to reveal the Curie point of produced samples, the temperature dependences of magnetization were collected in a magnetic field of 0.1 T (in field cooling regime for the whole series (Fig. 4)). The Curie temperature was revealed by calculations of the first derivative of the M vs T dependences measured for all samples. The estimated values of the T_C were 284 ± 1, 276 ± 1, 270 ± 1, 265 ± 1 K for $Mn_{0.97}W_{0.03}CoGe$, $Mn_{0.95}W_{0.05}CoGe$, $Mn_{0.93}W_{0.07}CoGe$, and $Mn_{0.9}W_{0.1}CoGe$, respectively. A gradual decrease in T_C was observed, which may be due to the reduction of the magnetic moment Mn by the addition of W. As it was mentioned above, the atomic radius of W is larger than Mn. It causes an increase in interatomic distances between Mn–Mn, Mn–Co, and Co–Co, which induces the weakening of exchange interactions and a decrease in the Curie temperature. Moreover, thermal hysteresis was not observed in all studied samples, which is also a confirmation of the occurrence of second-order phase transition in the produced materials [12].

The magnetocaloric effect is determined using indirect methods by calculating the change in magnetic entropy ΔS_M. These studies are based on magnetic isotherms measured over a wide range of temperatures. Maxwell's relations were used to calculate the change in magnetic entropy ΔS_M [13]

$$\Delta S_M(T, \Delta H) = \mu_0 \int_0^H \mathrm{d}H \left(\frac{\partial M(T,H)}{\partial T}\right)_H, \qquad (1)$$

where μ_0 is magnetic permeability, H is the magnetic field strength, M is the magnetization, and T is the temperature. The above equation (1) was implemented in Mathematica using the algorithm below [14]

$$\Delta S_M \frac{(T_i + T_{i+1})}{2} \approx \frac{1}{T_{i+1} - T_i} \left[\int_0^{B_{\max}} \mathrm{d}B\ M(T_{i+1}, B) - \int_0^{B_{\max}} \mathrm{d}B\ M(T_i, B) \right], \qquad (2)$$

where B is the magnetic field induction to the relation $B = \mu_0 H$.

The calculated temperature dependences of magnetic entropy change for all samples are presented in Fig. 5. The highest ΔS_M values calculated for a magnetic field change of ~ 5 T were 5.30, 4.16, 3.23, and 3.01 J/(kg K) for $Mn_{0.97}W_{0.03}CoGe$, $Mn_{0.95}W_{0.05}CoGe$, $Mn_{0.93}W_{0.07}CoGe$, and $Mn_{0.9}W_{0.1}CoGe$, respectively. Similarly to our previous work on the selective substitution of Mn by Zr [7] and Pd [8], the change in magnetic entropy was the largest for the Zr and Pd dopant content of $x = 0.05$. An increase in the content of the W addition causes a decrease in the value of the magnetic entropy change, which confirmed the results of measuring the Curie temperature. Moreover, a successive significant broadening of the ΔS_M peak with an increase in W content was

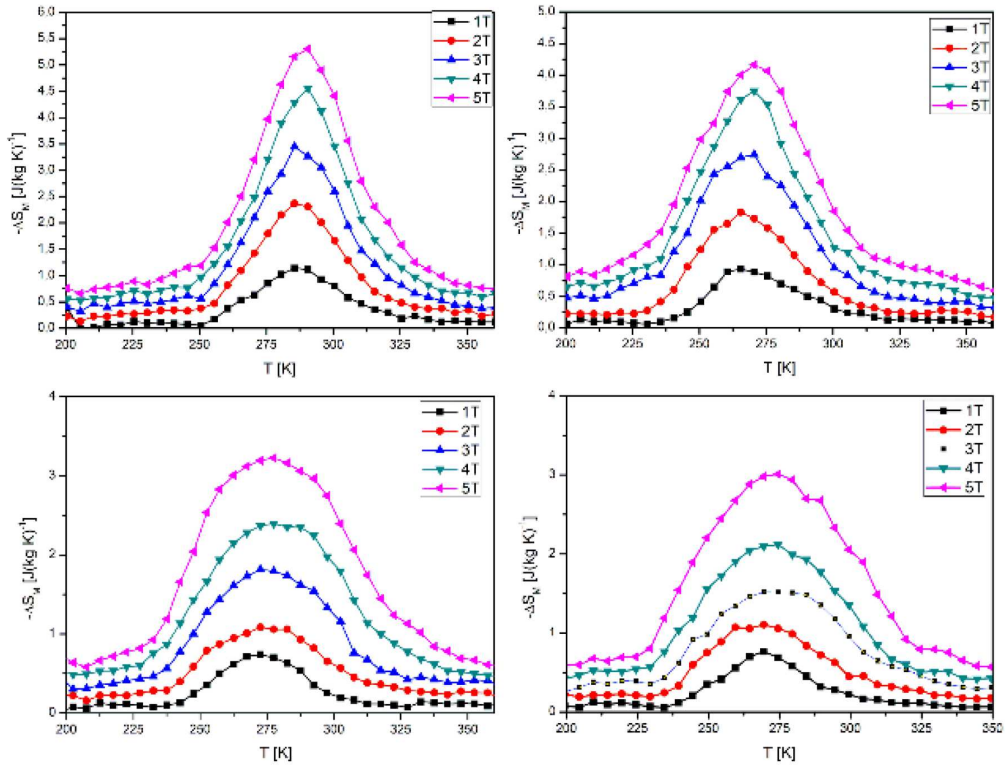

Fig. 5. The ΔS_M vs T curves revealed for $Mn_{0.97}W_{0.03}CoGe$ (a), $Mn_{0.95}W_{0.05}CoGe$ (b), $Mn_{0.93}W_{0.07}CoGe$ (c), and $Mn_{0.9}W_{0.1}CoGe$ (d) alloys.

noticed. Present results are much lower than those revealed for pure gadolinium, which is treated as a fundamental magnetocaloric material [15]. Such good properties of Gd are caused by the highest magnetic moment and the highest effective exchange coupling around room temperature [16]. Moreover, the results are also lower than those for MnCoGe modified by Fe or In addition, which is manifested by the fact that the ΔS_M value reached even 10.6 or 52 J/(kg K), respectively. The Curie temperature is comparable to those delivered in [17, 18].

Taking into account practical applications of MM'X alloys in domestic devices, the refrigeration capacity (RC) was calculated. The RC value was determined based on ΔS_M vs T curves using the following equation [19]

$$\mathrm{RC}\left(\delta T, H_{\max}\right) = \int_{T_{cold}}^{T_{hot}} \mathrm{d}T \; \Delta S_M\left(T, H_{\max}\right), \tag{3}$$

where RC is the refrigerant capacity, $\delta T = T_{hot} - T_{cold}$ is the temperature range of the thermodynamic cycle (δT corresponds to the full width at half maximum of magnetic entropy change peak), and $H_{\max}$ is the maximum value of the external magnetic field.

Calculations of the RC parameter revealed almost the same values for each produced alloy from the series. It is related to a systematic increase in full width at half maximum with a rise in W content, despite a decrease in maximum magnetic entropy change. The values of the change in magnetic entropy ΔS_M and the refrigeration capacity RC are summarized in Table II.

A relatively simple and fast method to study order phase transition was proposed by Law et al. in [20]. This technique uses a phenomenological field dependence of the magnetic entropy change, which could be written by following relation [20]

$$\Delta S_M = C\left(B_{\max}\right)^n, \tag{4}$$

where C is a constant depending on temperature and n is the exponent related to the magnetic state of the sample. Calculation of the exponent n by modifying (4) in the form proposed in [21] is as follows

$$\ln\left(\Delta S_M\right) = \ln(C) + n\ln\left(B_{\max}\right). \tag{5}$$

As shown in [22], the exponent n depends on the magnetic state of the material. If we assume that the tested material obeys the Curie–Weiss law, the exponent n should be $n = 1$ in the ferromagnetic state (below T_{C}) and $n = 2$ in the paramagnetic state (above T_{C}). Its value at T_{C} is strongly related to critical exponents and could be written in the following form

$$n = 1 + \frac{1}{\delta\left(1 - \frac{1}{\beta}\right)}, \tag{6}$$

where β and δ are critical exponents.

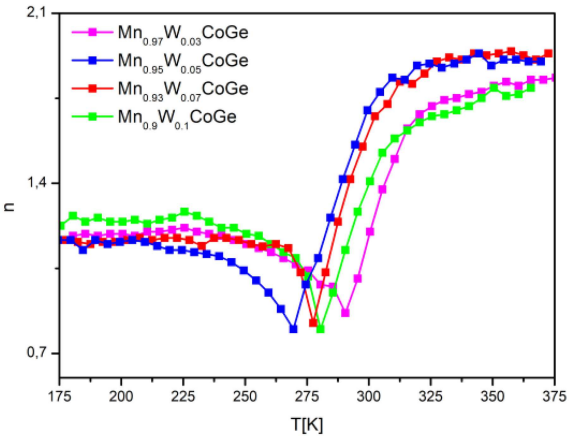

Fig. 6. Temperature dependence of the exponent n calculated for all tested (Mn,W)CoGe samples.

TABLE II

The magnetic entropy change ΔS_M and refrigeration capacity RC for the $Mn_{0.97}W_{0.03}CoGe$, $Mn_{0.95}W_{0.05}CoGe$, $Mn_{0.93}W_{0.07}CoGe$, and $Mn_{0.9}W_{0.1}CoGe$ alloys.

Sample	Magnetic field change $\Delta(\mu_0 H)$ [T]	Magnetic entropy change ΔS_M [J/(kg K)]	Refrigeration capacity RC [J/kg]
$Mn_{0.97}W_{0.03}CoGe$	1	1.14	32
	2	2.37	56
	3	3.45	74
	4	4.56	102
	5	5.30	134
$Mn_{0.95}W_{0.05}CoGe$	1	0.93	34
	2	1.83	58
	3	2.74	78
	4	3.75	104
	5	4.16	132
$Mn_{0.93}W_{0.07}CoGe$	1	0.74	33
	2	1.08	60
	3	1.82	76
	4	2.39	106
	5	3.23	135
$Mn_{0.9}W_{0.1}CoGe$	1	0.76	32
	2	1.11	64
	3	1.51	82
	4	2.12	108
	5	3.01	142

The n vs T curves for all tested samples are collected in Fig. 6. The shape of the n vs T curves constructed for the tested alloys with the addition of W is characteristic of the second type phase transition. A characteristic hump is observed near the Curie point value, which is typical for structural transformations similar to the results described in [23, 24]. The values of the exponent n revealed at the Curie point are 0.86, 0.79, 0.82, 0.79 for $Mn_{0.97}W_{0.03}CoGe$, $Mn_{0.95}W_{0.05}CoGe$, $Mn_{0.93}W_{0.07}CoGe$, and $Mn_{0.9}W_{0.1}CoGe$, respectively. These values are similar, which suggests that the values of critical exponents are close to others.

4. Conclusions

The research carried out in this work focused on the influence of partial substitution of Mn by W on the structure and thermomagnetic properties, as well as phase transitions of the tested MnCoGe alloys. XRD studies revealed the presence of two phases in all tested samples — an orthorhombic phase of the TiNiSi-type and a hexagonal phase of the Ni_2In-type with various W dopant contents. The detailed analysis of the X-ray diffraction pattern assisted by the Rietveld refinements did not reveal any structural transformation. The increase in the content of the addition of W at the expense of Mn in the tested alloys resulted in a decrease in the Curie temperature. A gradual decrease in magnetic entropy change with a rise of W in alloy composition was detected. The symmetrical shape of the temperature dependences of magnetic entropy change suggested second-order phase transition, which was confirmed by an analysis of n vs T curves constructed for the tested alloys. A course of all n vs T curves was independent of W content and characteristic of the second-order phase transition.

References

[1] E. Warburg, *Ann. Phys.* **13**, 141 (1881).

[2] P. Debye, *Ann. Phys.* **81**, 1154 (1926).

[3] W.F. Giauque, *J. Am. Chem. Soc.* **49**, 1864 (1927).

[4] V.K. Pecharsky, K.A. Gschneidner, Jr, *Phys. Rev. Lett.* **78**, 4494 (1997).

[5] G.J. Li, E.K. Liu, H.G. Zhang, Y.J. Zhang, J.L. Chen, W.H. Wang, H.W. Zhang, G.H. Wu, S.Y. Yu, *J. Magn. Magn. Mater.* **332**, 146 (2013).

[6] S. Lin, O. Tegus, E. Brück, W. Dagula, T. Gortenmulder, K. Buschow, *IEEE Trans. Magn.* **42**, 3776 (2006).

[7] K. Kutynia, P. Gębara, *Materials* **14**, 3129 (2021).

[8] K. Kutynia, A. Przybył, P. Gębara, *Materials* **16**, 539 (2023).

[9] P. Gębara, K. Kutynia, *Acta Phys. Pol. A* **135**, 298 (2019).

[10] W. Kraus, G. Nolze, *Powder Differ* **13**, 256 (1998).

[11] W. Bażela, A. Szytuła, J. Todorović, Z. Tomkowicz, A. Zięba, *Phys. Status Solidi A* **38**, 721 (1976).

[12] V.K. Pecharsky, K.A. Gschneider, Jr., *J. Appl. Phys.* **86**, 565 (1999).

[13] J. Świerczek, *J. Magn. Magn. Mater.* **322**, 2696 (2010).

[14] M.E. Wood, W.H. Potter, *Cryogenics* **25**, 667 (1985).

[15] A.M. Tishin, Y.I. Spichkin, *The Magnetocaloric Effect and its Application*, Institute of Physics Series in Condensed Matter Physics, 2003.

[16] S.K. Tripathy, K.G. Suresh, A.K. Nigam, *J. Magn. Magn. Mater.* **306**, 24 (2006).

[17] R.R. Wu, L.F. Bao, F.X. Hu et al., *Sci. Rep.* **5**, 18027 (2015).

[18] P. Gębara, M. Hasiak, *Materials* **14**, 185 (2021).

[19] A.O. Pecharsky, K.A. Gschneidner, V.K. Pecharsky, *J. Appl. Phys.* **93**, 4722 (2003).

[20] J.Y. Law, V. Franco, L.M. Moreno-Ramírez, A. Conde, D.Y. Karpenkov, I. Radulov, K.P. Skokov, O. Gutfleisch, *Nat. Commun.* **9**, 2680 (2018).

[21] V. Franco, A. Conde, V. Provenzano, R. Shull, *J. Magn. Magn. Mater.* **322**, 218 (2010).

[22] J. Świerczek, *Phys. Status Solidi A* **211**, 1567 (2014).

[23] K. Morrison, K.G. Sandeman, L.F. Cohen, C.P. Sasso, V. Basso, A. Barcza, M. Katter, J.D. Moore, K.P. Skokov, O. Gutfleisch, *Int. J. Refrig.* **35**, 1528 (2012).

[24] G.J. Li, E.K. Liu, H.G. Zhang, Y.J. Zhang, J.L. Chen, W.H. Wang, H.W. Zhang, G.H. Wu, S.Y. Yu, *J. Magn. Magn. Mater.* **332**, 146 (2013).